Investigation of turbulence and zonal flows for different shapes and scenarios in TCV using correlation ECE

V. Vuille[1], L. Porte[1], S. Brunner[1], S. Coda[1], A. Fasoli[1], Z. Huang[1],
C.A. de Meijere[1], G. Merlo[1], L. Vermare[2]

[1]*Centre de Recherches en Physique des Plasmas (CRPP), EURATOM/CH Association, EPFL, 1015 Lausanne, Switzerland*

[2]*École polytechnique, LPP, CNRS UMR 7648, 91128 Palaiseau cedex, France*

Introduction

Neoclassical transport theory systematically underestimates heat and particle transport in tokamak plasma. It is believed that turbulence is responsible for this [1]. Turbulence can also create global modes, like GAMs [2] [3], which in turn regulate its development, and therefore have a strong impact on transport. It is essential to characterise these phenomena and understand their creation and suppression mechanisms. These modes are spacially localized, of small amplitude and high frequency. By virtue of its high spatial and temporal resolution, correlation electron cyclotron emission (CECE) can be used to investigate the electron temperature component of turbulence in tokamaks.

Diagnostic: correlation ECE

A new 6-channel CECE radiometer has been installed on TCV. It uses spectral decorrelation as working principle [4]. Figure 1 presents the diagnostic, which has two perpendicular lines of sight at vertical position $z = 0$ and 21 cm. The RF stage is protected against ECRH reflected power (X2 & X3 harmonics), and includes an image reject highpass filter at 65 GHz, a mixer coupled with a 63 GHz local oscillator and IF amplification. The IF stage contains a 6-way power splitter, six remotely controlled bandpass YIG filters of range 6-18 GHz and bandwidth 170 MHz, another stage of amplification and six Schottky diodes. The signal goes through video cards with programmable gain and offset, and a fixed bandwidth of 450 kHz.

The spatial range of the radiometer goes from the low field side wall to the center of TCV. Ray tracing is used to reconstruct the plasma volume of emission. The radial resolution of 0.3-1.0 cm is mostly limited by relativistic effects, while the vertical resolution of 3-5 cm represents 95% of the gaussian beam entering the antenna. The acquisition frequency of the system is 1.75 MHz. Broadband turbulence in TCV usually appears in the frequency range 10 to 150 kHz. The 6 separated channels allow the simultaneous study of cross-spectra at 3 different locations or the computation of correlation length with only one discharge. Furthermore, TCV plasma can

be displaced vertically, providing access to poloidal angles in the range $[-\frac{\pi}{2}, \frac{\pi}{2}]$.

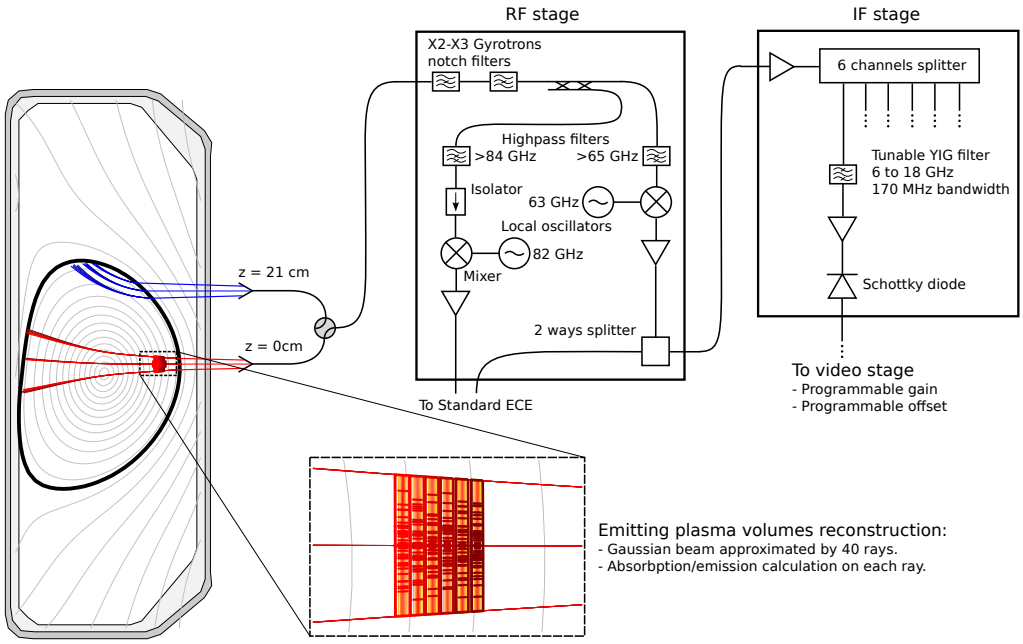

Figure 1: Scheme of the CECE diagnostic on TCV.

Triangularity effects on turbulence

In order to measure the effects of plasma triangularity on turbulence, several discharges[1] have been performed in both positive and negative δ. The six CECE channels have been probing in the gradient region: $\rho_\psi \in [0.5, 0.9]$. A spacing of ~ 0.4 cm between them allows a good decorrelation of the thermal noise and the measurement of cross-spectra and correlation lengths.

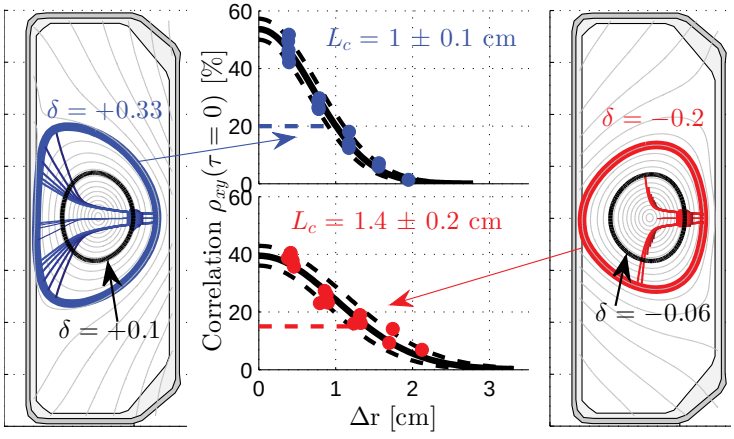

(a) Correlation length of turbulence for positive (#45721) and negative (#45728) triangularity. The **black** flux surface is $\rho_\psi = 0.69$ on both pictures.

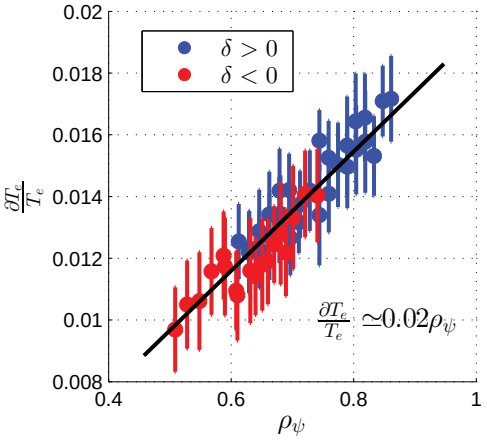

(b) Relative amplitude of the turbulence for both $\delta > 0$ and $\delta < 0$.

Figure 2: Summary of the triangularity study.

Two important differencies are to be noticed:

- The turbulence frequency range tends to be narrower for $\delta < 0$.
- The correlation length tends to be larger for $\delta < 0$ (figure 2a).

[1]Shots: #45719-20-21-22-23-24-27-28

However, the fluctuations relative amplitude, $\frac{\delta T_e}{T_e}$, is equivalent for both shapes in the measurement region (figure 2b), and seems to be linear with respect to ρ_ψ. Simulations show that negative triangularity should reduce the level of turbulence [5]. As shown on figure 2a, the elongation of positive δ shots is higher ($\kappa \approx 1.4$ against $\kappa \approx 1.2$). This could stabilize the turbulence and balance the weeker $\delta > 0$ confinement compared to $\delta < 0$. Also, the CECE measurements of turbulence for negative δ stop at $\rho_\psi < 0.75$, where the local triangularity is reduced to $\delta < -0.1$. Further study is required.

GAM detection

Geodesic acoustic modes have been simultaneously identified by 4 diagnostics on TCV:

- Tangential Phase Contrast Imaging $\rightarrow \tilde{n}_e$
- Mirnov coils (magnetics) $\rightarrow \tilde{B}_\theta$
- Doppler BackScattering $\rightarrow \tilde{v}_{E\times B}$
- Correlation ECE $\rightarrow \tilde{T}_e$

Although the dignostics do not probe at the same plasma volume, they all measure an oscillation at the frequency of 28 kHz (figure 3). The GAM can then be considered as a global mode. Furthermore, the phase of the mode is constant over the plasma (figure 4). This feature allows to use the TPCI or the magnetics as reference signal for synchronous detection with the six CECE channels. By this means, the uncorrelated turbulence is removed, emphasising the GAM. The complex coherence between the reference signal and a CECE channel (figure 5) can then be written:

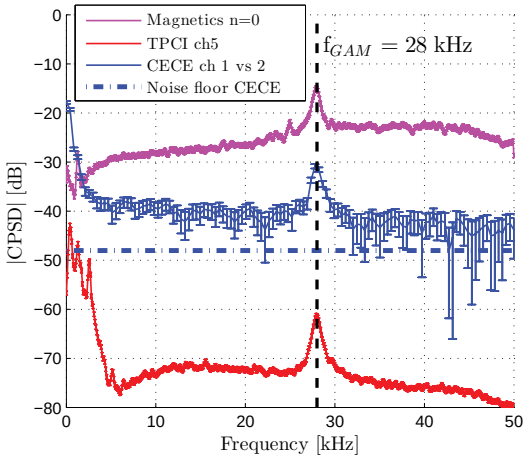

Figure 3: Power spectral density of TPCI, CECE and magnetics for shot #45891. A peak is observed at 28 kHz in all three diagnostics, even though they are not probing at the same location.

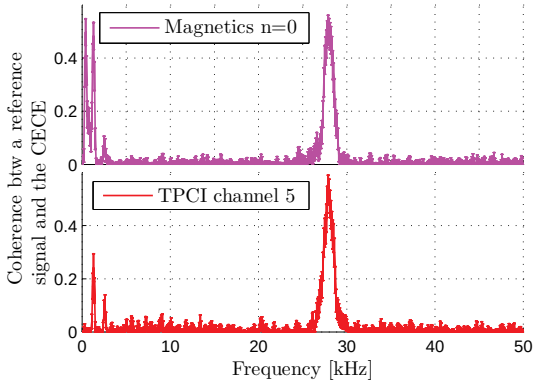

Figure 4: Coherence between magnetics/TPCI and CECE.

$$\gamma = \gamma_r + i\gamma_i = \cos(2\pi\frac{\Delta\rho_\psi}{\lambda_{GAM}} + \phi) + i\sin(2\pi\frac{\Delta\rho_\psi}{\lambda_{GAM}} + \phi)$$

where the fitted parameters λ_{GAM} and ϕ are respectively the wavelength of the GAM and a phase with respect to the reference. Here $\Delta\rho_\psi = \rho_{\psi,k} - \rho_{\psi,1}$, with k the CECE channel index. This method allows the computation of the GAM wavelength.

The GAM relative amplitude has been measured close to the LCFS (figure 6). It reaches a maximum near the edge: $\frac{\delta T_{rad}}{T_{rad}} \approx 0.6\%$ at $\rho_\psi = 0.98$. It then decreases quickly inside the plasma: $\frac{\delta T_{rad}}{T_{rad}} < 0.1\%$ at $\rho_\psi = 0.9$. As the optical depth at those locations is $\tau < 1$, the observed temperature, T_{rad}, is not equivalent to T_e. And the fluctuations can be approximated by [6]:

$$\frac{\delta T_{rad}}{T_{rad}} \approx 2\frac{\delta T_e}{T_e} + \frac{\delta n_e}{n_e}$$

Simulations with the gyrokinetic code GENE estimate the ratio $\frac{\delta n_e}{n_e}/\frac{\delta T_e}{T_e} \approx 0.5$ close to the LCFS in a comparable shot. δT_e is then responsible for $\sim 80\%$ of $\frac{\delta T_{rad}}{T_{rad}}$ and δn_e for $\sim 20\%$, which is not negligible. In order to properly estimate $\frac{\delta T_e}{T_e}$, direct measurements of $\frac{\delta n_e}{n_e}$ will be needed.

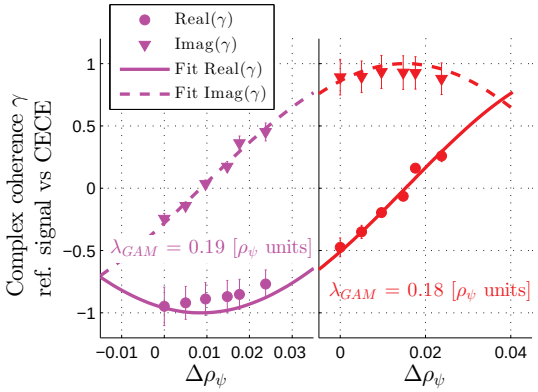

Figure 5: Wavelength measurement using the complexe coherence between a reference signal and the 6 CECE channels at the GAM frequency.

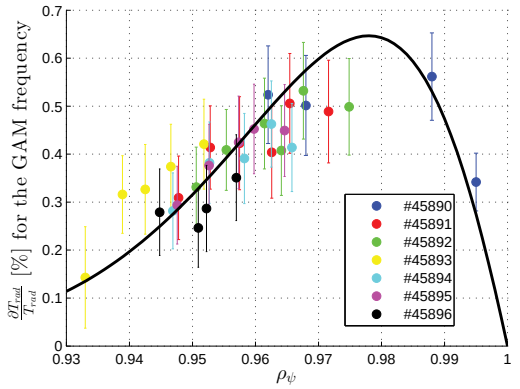

Figure 6: Relative amplitude of GAM oscillations seen by CECE.

Conclusion

Significant differences have been observed in the turbulent behaviour of positive and negative triangularity plasmas. However, elongation effects cannot be entirely separated from δ effects. More experiments are planned to clarify this issue.

A GAM has been identified using ECE radiometry. Its global nature allows a simultaneous measurement by TPCI, magnetics and CECE. Synchronous detection permits to remove the broadband turbulence and discriminate the GAM signal in the CECE. Edge ECE measurements are affected by density variations, but non-linear or quasilinear simulations can properly estimate the ratio $\frac{\delta n_e}{n_e}/\frac{\delta T_e}{T_e}$ and separate both components. The quasilinear approximation shall become a standard tool in the interpretation of CECE data.

Acknowledgement

This work was partly supported by the Fonds National Suisse pour la Recherche Scientifique.

References

[1] A.J. Wootton *et al.*, Phys. Fluids B **2**, 2879 (1990)

[2] P.H. Diamond *et al.*, Plasma Phys. Control. Fusion **47**, (2005)

[3] K. Itoh *et al.*, Plasma and Fusion Research **1**, 037 (2006)

[4] C. Watts, Fusion Science and Technology **52**, Aug. (2007)

[5] A. Marinoni *et al.*, Plasma Phys. Control. Fusion **51**, (2009)

[6] T.D. Rempel *et al.*, Rev. Sci. Instrum. **65**, 2044 (1994)